Magnetic, Spectroscopic, and Structural Studies of Dicobalt Hydroxamates and Model Hydrolases[||]

David A. Brown,*,[†] W. Errington,[‡] W. K. Glass,[†] W. Haase,[§] T. J. Kemp,[‡] H. Nimir,[†] S. M. Ostrovsky,[§] and R. Werner[§]

Department of Chemistry, University College Dublin, Belfield, Dublin 4, Ireland, Department of Chemistry, University of Warwick, Coventry CV4 7AL, U.K., and Institut für Physikalische Chemie, Technische Universität, Darmstadt, Germany

Received March 27, 2001

The cobalt(II) urease model complex $[Co_2(\mu\text{-OAc})_3(\text{urea})(\text{tmen})_2][\text{OTf}]$ (**2**) prepared from the cobalt model hydrolase $[Co_2(\mu\text{-H}_2\text{O})(\mu\text{-OAc})_2(\text{OAc})_2(\text{tmen})_2]$ (**1**) undergoes facile reaction with acetohydroxamic acid (AHA) to give the monobridged hydroxamate complex $[Co_2(\mu\text{-OAc})_2(\mu\text{-AA})(\text{urea})(\text{tmen})_2][\text{OTf}]$ (**3**) while **1** gives the dibridged hydroxamate complex $[Co_2(\mu\text{-OAc})(\mu\text{-AA})_2(\text{tmen})_2][\text{OTf}]$ (**4**). The structures and Co−Co distances of the hydroxamate derivatives of **1** and **2** are very close to those of their nickel analogues and suggest that hydroxamic acids can also inhibit cobalt-based hydrolases as well as inhibiting urease. **1** also reacts with glutarodihydroxamic acid (gluH_2A_2) to eliminate hydroxylamine with formation of $[Co_2(\mu\text{-OAc})_2\{\mu\text{-O(N)(OC)}_2(\text{CH}_2)_3\}(\text{tmen})_2][\text{OTf}]$ (**5**), the structure of which is very close to that of its nickel analogue. Both **1** and **3** show weak antiferromagnetic coupling. Oxidation of **1** with H_2O_2 gives three dicobalt(III) hydroxy complexes (**7**−**9**), the first of which $[Co_2(\mu\text{-OAc})_2(\text{OAc})_2(\mu\text{-OH})(\text{tmen})_2][\text{OTf}]$ (**7**) contains a bridging hydroxyl and the second $[Co_2(\mu\text{-OAc})_2(\text{OAc})(\mu\text{-OH})(\text{OH})(\text{tmen})_2][\text{OTf}]$ (**8**) containing both a bridging and terminal hydroxyl, while the third $[Co_2(\mu\text{-OAc})(\text{OAc})_2(\mu\text{-OH})_2(\text{tmen})_2][\text{OTf}]$ (**9**) contains two bridging OH groups with mixed-valence Co(II)/(Co(III) intermediates.

Introduction

Dinuclear metallohydrolases are an important group of metalloenzymes which catalyze the hydrolysis of a range of peptide and phosphate ester bonds and include the amidohydrolases, amidinohydrolases, and peptide hydrolases.[1] A common structural feature of these metallohydrolases is a dinuclear metal active site featuring Zn(II), Ni(II), Co(II), and Mn(II) and carboxylate bridges which occur respectively in leucine aminopeptidase,[2] urease,[3] methionine aminopeptidase,[4] and arginase.[5] Although crystal structural data are now available for these metallohydrolases,[2−5] the mechanism involved in their catalytic hydrolysis of various substrates is still a matter for discussion. The generally accepted mechanism is based on that first proposed by Zerner[6] for the action of urease in which one nickel(II) center activates the urea substrate by coordination of the carbonyl oxygen while the other nickel center coordinates a water molecule which is deprotonated by a suitably oriented base of the protein to produce a hydroxide which then attacks the activated urea carbonyl carbon atom to give a tetrahedral intermediate which decomposes to give eventually ammonia and carbon dioxide.

One problem in mechanistic discussions based on structural evidence is the uncertainty in the protonation state of the solvent water molecule; that is, is it a neutral molecule, a hydroxide, or even a bridging oxide? More recent discussions stress the importance of hydrogen bonding to various amino acid residues by the amino hydrogens of the urea substrate[7] although controversy remains since it has recently been suggested that one of the amino groups of urea approaches the six- coordinated Ni(II) center and eventually bridges the two nickel centers, thereby polarizing the C−O and $C-NH_2$ bonds and assisting nucleophilic attack.[8] Some support for this mechanism is provided by the isolation of complexes such as $[L_2Ni_2(\mu\text{-OAc})(\text{urea})](ClO_4)_2$ (L = pyrazolate derivative), where H bonding by the NH_2 groups to an oxygen atom of a bridging carboxylate is confirmed by structural data.[9] Most recently, it has been suggested on the basis of model studies that hydrolysis of urea at a dinickel center may proceed through initial elimination of ammonia from the coordinated urea molecule followed by hydrolysis of the resulting bridged cyanate complex.[10] In other cases, e.g. methionine aminopeptidase (MAP) and arginase, the mechanisms of hydrolysis are not clear but presumed to be based

* Author for correspondence.
[†] University College Dublin.
[‡] University of Warwick.
[§] Technische Universität.

[||] Abbreviations: OAc, CH_3COO^-; tmen, *N*,*N*,*N*′,*N*′-tetramethylethylenediamine; TMS-OTf, (trimethylsilyl)triflate; OTf (triflate), $CF_3SO_3^-$; AHA, acetohydroxamic acid; AA, acetohydroxamate anion; gluH_2A_2, glutarodihydroxamic acid; gluA_2, glutarodihydroxamate dianion.

(1) Wilcox, D. E. *Chem. Rev.* **1996**, *96*, 2435−2458.
(2) Sträter, N.; Lipscomb, W. N. *Biochemistry* **1995**, *34*, 14792−14800.
(3) Jabri, E.; Carr, M. B.; Hausinger, R. P.; Karplus, P. A. *Science* **1995**, *268*, 998−1004.
(4) Roderick, S. L.; Matthews, B. W. *Biochemistry* **1993**, *32*, 3907−3912.
(5) Kanyo, Z. F.; Scolnick, L. R.; Ash, D. E.; Christianson, D. W. *Nature* **1996**, *383*, 554−557.
(6) Dixon, N. E.; Riddles, C.; Gazzola, C.; Blakely, R. L.; Zerner, B. *Can. J. Biochem.* **1980**, *58*, 1335−1345.
(7) Karplus, P. A.; Pearson, M. A.; Hausinger, R. P. *Acc. Chem. Res.* **1997**, *30*, 330−37.
(8) Benini, S.; Rypniewski, W. R.; Wilson, K. S.; Miletti, S.; Ciurli, S.; Mangani, S. *Structure* **1999**, *7*, 205−216.
(9) Konrad, M.; Meyer, F.; Jacobi, A.; Kircher, P.; Rutsch, P.; Zsolnai, L. *Inorg. Chem.* **1999**, *38*, 4559−4566.
(10) Barrios, A. M.; Lippard, S. J. *J. Am. Chem. Soc.* **2000**, *122*, 9172−9177.

10.1021/ic0103345 CCC: $20.00
Published on Web 10/12/2001

on the Zerner scheme.[5] The inhibition of metalloenzymes is also of current interest especially because of possible therapeutic applications. For example, the inhibition of matrix metalloproteinases by various hydroxamate-based inhibitors generally involves chelation of a mononuclear zinc center by the hydroxamate function.[11] Hydroxamic acids are also potent inhibitors of urease,[12] but in this case the structure of the acetohydroxamate-inhibited C319A variant of *Klebsiella aerogenes* urease shows the deprotonated hydroxyl oxygen of the hydroxamic acid bridging the two nickel centers with the carbonyl oxygen bonding one nickel center only[13] in contrast to normal O,O chelation of a metal ion by a hydroxamic acid. A similar structure is found in the dizinc metalloenzyme *Aeromonas proteolytica* aminopeptidase Zn_2 AAP inhibited by *p*-iodo-D-phenylalanine hydroxamic acid.[14]

These dinuclear metalloenzymes often exchange metal ions within the above sequence with varying effects on their activities with respect to various substrates. For example, exchange of Ni(II) by Zn(II) or Co(II) in urease results in a large decrease in activity with urea[15] and similarly replacement of Ni(II) by Mn(II) in urease also results in a marked decrease in activity with urea.[5] In contrast, substitution of 2 mol atoms of Zn in Zn_2AAP by Co(II), Cu(II), and Ni(II) gives hyperactive substituted enzymes with rate enhancements of 6.5, 7.7, and 25, respectively, in reactivity compared to that of the parent zinc enzyme with certain substrates. Moreover, addition of 1 mol of these ions to apo-AAP followed by equilibration and then addition of 1 mol of the second metal ion gives a discrete heterodimetallic site that is also enzymatically active.[16] In previous papers,[17,18]we have attempted to model the inhibition of urease by hydroxamic acids by the reactions of acetohydroxamic acid (AHA) with the model complex $[Ni_2(\mu\text{-OAc})_3(\text{urea})(\text{tmen})_2][\text{OTf}]$ (**A**), which reacts rapidly with acetohydroxamic acid (AHA) to give the monobridged hydroxamate complex $[Ni_2(\mu\text{-OAc})_2(\mu\text{-AA})(\text{urea})(\text{tmen})_2][\text{OTf}]$ with a structure very similar to that of the acetohydroxamate inhibited C319A variant of *Klebsiella aerogenes* urease.[13]

In view of the use of a number of dinuclear divalent metal centers, $[Zn(II)]_2$, $[Ni(II)]_2$, and $[Mn(II)]_2$ by metallohydrolases and their ability to exchange metals ions within this sequence, we have extended our previous modeling of ureases[17,18] to related dicobalt(II) systems and their reactions with hydroxamic acids as possible models for methionine aminopeptidase (MAP) which has been proved by a crystal structure determination to contain a dicobalt center and to be inhibited by various reagents including epoxides although the position with regard to inhibition by hydroxamic acids is not clear; however, the above dizinc metalloenzyme, *Aeromonas proteolytica* aminopeptidase, Zn_2-AAP, is clearly inhibited by *p*-iodo-D-phenylalanine hydroxamic acid with a structure similar to that of the inhibited urease[14] and the above model complex.[17]

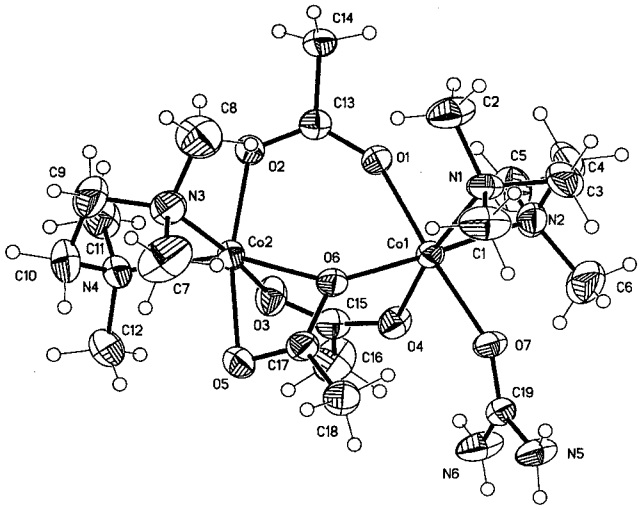

Figure 1. Molecular structure of the cation of dicobalt(II) complex **2,** $[Co_2(\mu\text{-OAc})_3(\text{urea})(\text{tmen})_2]^+$.

As discussed above, it was decided to attempt the synthesis of model dicobalt(III) complexes with bridging hydroxo groups by oxidation of the model dicobalt(II) complexes and compare their behavior with those containing bridging water molecules.

Results and Discussion

The cobalt(II) analogue (**2**) of the urease model complex, $[Ni_2(OAc)_3(\text{urea})(\text{tmen})_2][\text{OTf}]$,[19] was prepared similarly from the previously reported $[Co_2(\mu\text{-}H_2O)(\mu\text{-OAc})_2(OAc)_2(\text{tmen})_2]$ (**1**)[20] by its reaction with urea in dichloromethane in the presence of triflate. The monobridged hydroxamate cobalt dimer $[Co_2(\mu\text{-OAc})_2(\mu\text{-AA})(\text{urea})(\text{tmen})_2][\text{OTf}]$ (**3**) was prepared by the reaction of acetohydroxamic acid (AHA) with **2** in a 1:1 ratio in dichloromethane. The dibridged acetohydroxamate complex $[Co_2(\mu\text{-OAc})(\mu\text{-AA})_2(\text{tmen})_2][\text{OTf}]$ (**4**) was obtained as pink crystals by the reaction of **1** with acetohydroxamic acid in a 2:1 molar ratio in acetone in the presence of triflate. As in the analogous nickel(II) complexes,[17] the above reactions are facile and occur very rapidly at room temperature and in other solvents such as methanol. Reaction of **1** with glutarodihydroxamic acid, $(CH_2)_3(CONHOH)_2$, $gluH_2A_2$, at room temperature in methanol in the presence of triflate gave $[Co_2(\mu\text{-OAc})_2\{\mu\text{-O(N)(OC)}_2\text{-}(CH_2)_3\}(\text{tmen})_2][\text{OTf}]$ (**5**) which contains a deprotonated bridging *N*-hydroxyglutarimide (Figure 4) as in the analogous dinickel complex.[18]

Crystal Structures of 2−5. The crystal structures of the urea adduct $[Co_2(\mu\text{-OAc})_3(\text{urea})(\text{tmen})_2][\text{OTf}]$ (**2**), the monobridged acetohydroxamate complex $[Co_2(\mu\text{-OAc})_2(\mu\text{-AA})(\text{urea})(\text{tmen})_2][\text{OTf}]$ (**3**), the dibridged acetohydroxamate complex $[Co_2(\mu\text{-OAc})(\mu\text{-AA})_2(\text{tmen})_2][\text{OTf}]$ (**4**), and the deprotonated *N*-hydroxyglutarimide-bridged complex $[Co_2(\mu\text{-OAc})_2\{\mu\text{-O(N)(OC)}_2\text{-}(CH_2)_3\}(\text{tmen})_2][\text{OTf}]$ (**5**) are shown in Figures 1−4, respectively, with crystallographic data in Table 1 and selected bond lengths and angles in Tables 2−5, respectively. In all four complexes, the structures shown in Figures 1−4 are very close to those of the corresponding nickel complexes,[17,18] with the acetohydroxamate bridging groups in both the mono- and

(11) Beckett, R. P.; Davidson, A. H.; Drummond, A. H.; Huxley, P.; Whitetaker, M. *Drug Discovery Today* **1996**, *1*, 16−26
(12) Karger, S. In *Chemistry and Biology of Hydroxamic Acids*; Kehl, H., Ed.; Basel, 1982.
(13) Pearson, M. A.; Michel, L, O.; Hausinger, R. P.; Karplus, P. A.; *Biochemistry* **1997**, *36*, 8164−8172.
(14) Chevrier, B.; D'Orchymoant, H.; Schalk, C.; Tamus, C.; Moras D. *Eur. J. Biochem*. **1996**, *237*, 393−398.
(15) King, G. J.; Zerner, B. *Inorg. Chim. Acta* **1997**, *255*, 381−388.
(16) Prescot, J. M.; Wagner, F. W.; Holmquist, B.; Vallee, B. L. *Biochem. Biophys. Res. Commun*. **1983**, *114*, 646−652.
(17) Arnold, M.; Brown, D. A.; Deeg, O.; Errington, W.; Haase, W.; Herlihy, K.; Kemp, T. J., Nimir, H.; Werner R. *Inorg. Chem*. **1998**, *37*, 2920−2928.
(18) Brown, D. A.; Cuffe, L. P., Deeg, O.; Errington, W.; Fitzpatrick, N. J.; Glass, W. K.; Herlihy, K.; Kemp, T. J.; Nimir. H. *J. Chem. Soc., Chem. Commun*. **1998**, 2433−2434.
(19) Wages, H. E.; Taft, K. L.; Lippard, S. J. *Inorg. Chem*. **1993**, *32*, 4985−4987.
(20) Turpeinein, U.; Hämäläinen, R.; Reedijk, J. *Polyhedron* **1987**, *6*, 1603−1610.

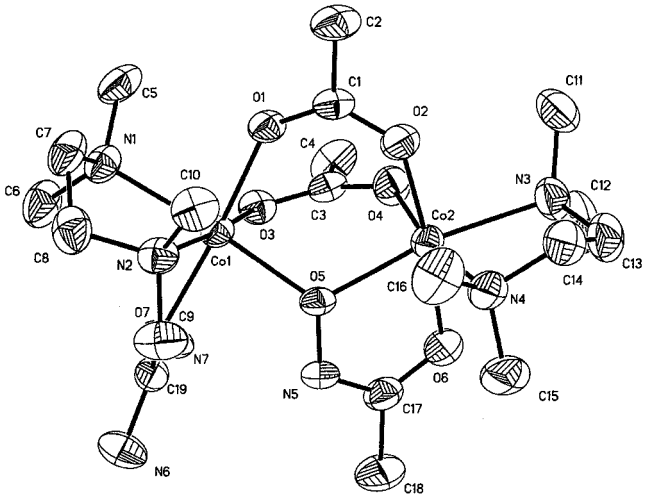

Figure 2. Molecular structure for the cation of dicobalt(II) monobridged acetohydroxamate complex **3**, $[Co_2(\mu\text{-}OAc)_2(\mu\text{-}AA)(urea)(tmen)_2]^+$.

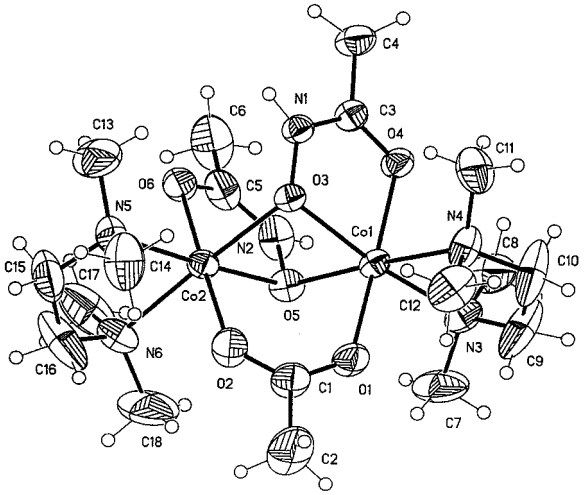

Figure 3. Molecular structure for the cation of dicobalt(II) dibridged acetohydroxamate complex **4**, $[Co_2(\mu\text{-}OAc)(\mu\text{-}AA)_2(tmen)_2]^+$.

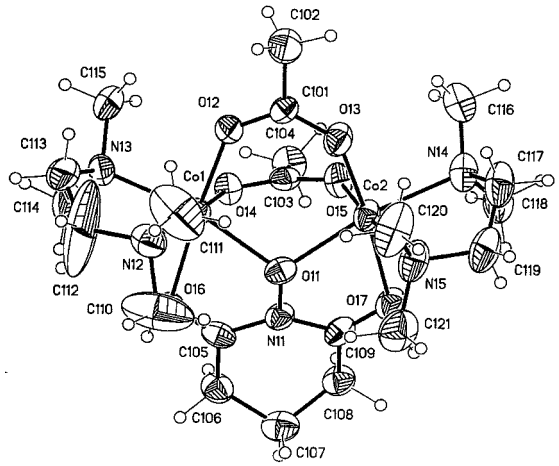

Figure 4. Molecular structure for the cation of dicobalt(II) complex **5**, $[Co_2(\mu\text{-}OAc)_2\{\mu\text{-}O(N)(OC)_2(CH_2)_3\}(tmen)_2]^+$.

dibridged complexes, **3** and **4** and **I** and **II**,[17] exhibiting exactly the same coordination modes in both the dicobalt and dinickel series. In all cases, the deprotonated hydroxamate hydroxyl oxygen bridges the two metal centers while the carbonyl oxygen coordinates only one metal center.

The coordination about the cobalt atoms in **3** is distorted octahedral compared to the parent compound **2** (Figure 2); for example in complex **3**, O(5)−Co(1)−O(1) is 94.10(6)° whereas the equivalent angle O(1)−Co(l)−O(6) in **2** is 90.89(6)°. As a consequence of forming only a single acetohydroxamate bridge in **3** by simple replacement of the monodenate bridging acetate in **2**, the Co---Co distance in **3** is 3.4316(17) Å (Table 3), which is greater than that in the native dicobalt MAP, 2.9 Å, but is close to that in the parent compound **2**, 3.4813(3) Å, and slightly less than that in the hydroxamate inhibited dizinc *Aeromonas proteolytica* aminopeptidase Zn_2AAP, 3.7 Å.[14] The urea molecule remains coordinated via its oxygen atom O(7) to Co(1), and there is a slight increase in the Co(1)−O(7)(urea) distance in **3**, 2.1406(16) Å, compared to 2.0978(14) Å in the parent complex **2**. This may indicate a decrease in the metal Lewis acidity upon hydroxamate coordination compared to acetate coordination, which is consistent with the inhibition of metal-dependent hydrolases by hydroxamic acids. Figure 3 shows the structure obtained for the cation of **4**. In this molecule, hydroxamate coordination results in the loss of one of the bridging acetates, both terminal acetates, and the bridging water molecule in **1**. The hydroxamate moieties are bound in a similar manner as in **3**, by using the deprotonated oxygens, O(3) and O(5), as bridging atoms and carbonyl oxygens, O(4) and O(6), as monodentate atoms. Both cobalt atoms in **4** are in a distorted octahedral environment which is exemplified by the angles O(1)−Co(1)−O(3) of 97.96(10)° and O(2)−Co(2)−O(5) of 95.69(11)° (Table 4). The formation of two acetohydroxamate bridges in **4** results in a decrease in the Co---Co distance to 3.0971(6) Å compared to 3.4316(17) Å in **3**, but it is close to that reported for the related dinickel dibridged salicylhydroxamate urease model of 3.016 Å.[21] The ability of cobalt(II) to form a series of complexes analogous to those of nickel(II), including formation of hydroxamate-bridged complexes and elimination of hydroxylamine from glutarodihydroxamic acid, is in accord with studies of the exchange of metal(II) centers within metalloenyzmes as noted in the Introduction. The formation of the bridged hydroxamate complexes (**3** and **4**) suggests inhibition of dicobalt-based metalloenzymes similar to that observed in the acetohydroxamate complex with the C319A variant of urease involving a dinickel-bridged hydroxamate structure and the very similar dizinc-bridged structure in the *p*-iodo-d-phenylalanine hydroxamate complex with *Aeromonas proteolytica* aminopeptidase AAP.[14] In the case of the closely related methionine aminopeptidase containing a dicobalt active site with approximately octahedral coordination of the Co(II) centers by both carboxylate and a histidine nitrogen,[4] inhibition by the epoxide-containing compounds fumagillin and ovalicin occurs by modification of a histidine center although there is spectroscopic evidence for some interaction at the dicobalt center.[22] The above expoxides also inhibit angiogenesis which may be therapeutically important, and the related compound TNP-470 is currently on trial as an anticancer reagent. However, to date, inhibition of MAP by hydroxamic acids has not been structurally characterized.

The crystal structure of the *N*-hydroxyglutarimide dicobalt **5** (Figure 4) shows that the deprotonated N−OH oxygen of the *N*-hydroxyglutarimide residue O(11) bridges the two cobalt ions Co(1) and Co(2) and the two carbonyl oxygens O(16) and O(17) coordinate to their respective cobalt atoms Co(1) and Co(2).

(21) Stemmler, A. J.; Kampt, J. W.; Kirk, M. L.; Pecoraro, V. L. *J. Am. Chem. Soc.* **1995**, *117*, 6368−6369.
(22) Lowther, T. W.; McMillen, D. A.; Orville, A. M.; Matthews, B. W. *Proc. Natl. Acad. Sci. U.S.A.* **1998**, *95*, 12153−12157.

Table 1. Crystal Data and Structure Refinement for Compounds **2**−**5** and **7**−**9**

param	**2**	**3**	**4**	**5**	**7**	**8**	**9**
Formula	$C_{20}H_{45}Co_2F_3N_6O_{10}S$	$C_{20}H_{46}Co_2F_3N_7O_{10}S$	$C_{19}H_{45}Co_2F_3N_6O_{10}S$	$C_{22}H_{44}Co_2F_3N_5O_{10}S$	$C_{21}H_{45}Co_2F_3N_4O_{12}S$	$C_{19}H_{43}Co_2F_3N_4O_{11}S$	$C_{19}H_{43}F_3Co_2N_4O_{11}S$
M_r	736.54	751.56	724.53	745.54	752.53	710.29	710.29
cryst system	Triclinic	monoclinic	triclinic	triclinic	monoclinic	monoclinic	monoclinic
space group	$P\bar{1}$	$P2_1/c$	$P\bar{1}$	$P\bar{1}$	$P2_1/c$	$P2_1/n$	$P2_1/c$
a/Å	9.7021(1)	11.0745(6)	10.4771(5)	10.7949(8)	8.3982(3)	8.5756(6)	8.0482(9)
b/Å	11.5985(2)	13.6540(7)	11.4398(6)	15.7459(10)	13.2386(6)	22.1861(12)	29.076(3)
c/Å	15.2967(3)	22.6864(11)	14.9218(7)	20.9128(18)	29.0771(6)	16.4845(12)	12.8882(14)
α/deg	101.921(1)	90	77.148(1)	74.076(2)	90	90	90
β/deg	95.710(1)	94.47(3)	81.757(1)	84.566(3)	95.698(3)	100.936(3)	93.965(3)
γ/deg	96.481(1)	90	71.299(1)	81.201(3)	90	90	90
V/Å^3	1660.04(5)	3420.0(3)	1646.57(14)	3372.8(4)	3216.8(2)	3079.4(4)	3008.8(6)
T/K	180(2)	180(2)	180(2)	180(2)	180(2)	180(2)	180(2)
Z	2	4	2	4	4	4	4
λ/Å	0.710 73	0.710 73	0.710 73	0.710 73	0.710 73	0.710 73	0.710 73
ρ(calcd)/Mg m^{-3}	1.474	1.460	1.461	1.468	1.554	1.533	1.568
cryst size/mm	0.30 × 0.30 × 0.30	0.40 × 0.38 × 0.12	0.40 × 0.30 × 0.14	0.30 × 0.20 × 0.20	0.30 × 0.24 × 0.10	0.40 × 0.10 × 0.04	0.20 × 0.20 × 0.20
μ/mm^{-1}	1.133	1.103	1.141	1.116	1.174	1.219	1.248
hkl ranges	−12, 12; −14, 10; −20, 19	−14, 11; −14, 17; −29, 30	−12, 8; −14, 13; −18, 18	−14, 13; −21, 20; −27, 17	−11, 10; −9, 17; −35, 38	−10, 10; −26, 23; −11, 19	−9, 9;−34, 23; 15, −15
no. of reflcns collcd	9900	20 291	8971	20 461	19 711	15 801	15 319
indepdt reflcns	7200 (R_{int} = 0.0197)	8065 (R_{int} = 0.023)	6276 (R_{int} = 0.016)	14 888 (R_{int} = 0.003)	7796 (R_{int} = 0.045)	5428 (R_{int} = 0.047)	5285 (R_{int} = 0.037)
max and min transm	0.7618, 0.8437	0.8791, 0.6668	0.8566, 0.6582	0.8076, 0.7307	0.9165, 0.6364	0.9528, 0.6412	0.8312, 0.6716
$R(F)$ [$I > 2\sigma(I)$]/%	3.40	3.94	4.80	8.28	4.21	4.63	6.95
$R_w(F^2)$ (all data)/%	7.90	9.66	12.53	20.79	9.30	11.40	18.90
goodness of fit on F^2	0.905	1.065	1.064	1.071	1.004	1.031	1.048
largest peak and hole/e Å^{-3}	0.412, −0.790	0.623, −0.542	0.958, −0.548	1.296, −1.058	0.390, −0.636	0.529, −0.427	1.838, −0.739

Table 2. Selected Bond Lengths (Å) and Angles (deg) for Complex **2**

Co(1)−Co(2)	3.4813(3)	Co(1)−O(4)	2.076(2)
Co(1)−O(7)	2.0978(14)	Co(1)−O(1)	2.0815(14)
Co(1)−N(1)	2.209(2)	Co(1)−O(6)	2.140(2)
Co(2)−O(2)	2.009(2)	Co(1)−N(2)	2.215(2)
Co(2)−N(4)	2.144(2)	Co(2)−O(3)	2.070(2)
Co(2)−O(6)	2.1875(14)	Co(2)−O(5)	2.155(2)
Co(2)−C(17)	2.519(2)	Co(2)−N(3)	2.279(2)

O(4)−Co(1)−O(1)	94.76(6)	O(4)−Co(1)−O(7)	89.84(6)
O(1)−Co(1)−O(7)	175.16(6)	O(4)−Co(1)−O(6)	92.29(6)
O(1)−Co(1)−O(6)	90.89(6)	O(7)−Co(1)−O(6)	90.41(6)
O(4)−Co(1)−N(1)	171.46(7)	O(2)−Co(2)−O(3)	91.83(7)
O(7)−Co(1)−N(1)	85.40(6)	O(3)−Co(2)−N(4)	88.51(8)
O(4)−Co(1)−N(2)	89.98(7)	O(3)−Co(2)−O(5)	92.77(7)
O(7)−Co(2)−N(2)	91.19(7)	O(2)−Co(2)−O(6)	103.47(6)
O(2)−Co(2)−O(5)	163.67(6)	O(5)−Co(2)−N(3)	90.51(7)
N(4)−Co(2)−O(5)	95.25(7)	O(2)−Co(2)−C(17)	134.03(7)
O(3)−Co(2)−O(6)	96.64(6)	N(4)−Co(2)−C(17)	124.88(8)
O(5)−Co(2)−O(6)	60.42(6)	O(6)−Co(2)−C(17)	30.64(6)
O(3)−Co(2)−N(3)	170.77(7)		

Table 3. Selected Bond Lengths (Å) and Angles (deg) for Complex **3**

Co(1)−Co(2)	3.4316(17)	Co(1)−O(3)	2.0774(17)
Co(1)−O(1)	2.0813(16)	Co(1)−O(5)	2.0779(16)
Co(1)−N(1)	2.219(2)	Co(1)−O(7)	2.1406(16)
Co(2)−O(2)	2.0523(18)	Co(1)−N(2)	2.260(2)
Co(2)−O(5)	2.0840(16)	Co(2)−O(4)	2.0802(17)
Co(2)−N(3)	2.199(2)	Co(2)−O(6)	2.0986(18)
Co(2)−N(4)	2.245(2)		

O(3)−Co(1)−O(5)	95.49(6)	O(3)−Co(1)−O(1)	93.75(7)
O(5)−Co(1)−O(1)	94.10(6)	O(3)−Co(1)−O(7)	89.83(6)
O(5)−Co(1)−O(7)	88.61(6)	O(1)−Co(1)−O(7)	175.27(7)
O(3)−Co(1)−N(1)	91.57(7)	O(5)−Co(1)−N(1)	172.71(8)
O(1)−Co(1)−N(1)	87.20(7)	O(1)−Co(1)−N(1)	89.62(7)
O(3)−Co(1)−N(2)	172.63(7)	O(5)−Co(1)−N(2)	91.18(7)
O(1)−Co(2)−N(2)	88.88(7)	O(7)−Co(1)−N(2)	87.20(7)
N(1)−Co(1)−N(2)	81.67(8)	O(2)−Co(2)−O(4)	92.42(7)
O(2)−Co(2)−O(5)	95.06(7)	O(4)−Co(2)−O(5)	97.96(7)
O(2)−Co(2)−O(6)	174.28(8)	O(4)−Co(2)−O(6)	88.53(8)
O(5)−Co(2)−O(6)	79.22(7)	O(2)−Co(2)−N(3)	92.92(9)
O(4)−Co(2)−N(3)	87.87(8)	O(5)−Co(2)−N(3)	169.89(8)
O(6)−Co(2)−N(3)	92.76(9)	O(2)−Co(2)−N(4)	86.62(8)
O(4)−Co(2)−N(4)	169.83(8)	O(5)−Co(2)−N(4)	92.21(8)
O(6)−Co(2)−N(4)	93.43(8)	N(3)−Co(2)−N(4)	82.07(9)

Formation of **5** involves the novel elimination of hydroxylamine. We suggest that the two cobalt(II) centers in **5** act as Lewis acids polarizing both carbonyl groups of glutarodihydroxamic acid; protonation of one of the hydroxamate nitrogens and subsequent attack by the nucleophilic nitrogen at the other end of the dihydroxamic acid leads to the loss of the NH_2OH group, ring closure, and formation of a tetrahedral intermediate, which collapses on release of a proton and formation of **5** as proposed for the nickel analogue.[18] This mechanism is related to that proposed for the cleavage of the C−N bond in peptide hydrolysis catalyzed by a dizinc center in aminopeptidases, in particular that proposed for the hydrolysis of an N-terminal amino acid at bILAP.[2]

Spectroscopic Studies. The electronic spectra of **2**−**5** measured in CH_2Cl_2 are very similar and typical of a distorted octahedral environment about a Co(II) center with bands in the visible region at ca. 525 nm assigned to the $^4T_{1g}(F) \rightarrow {}^4T_{1g}(P)$ transition and in the near-infrared region at ca. 1090 nm assigned to the $^4T_{1g}(F) \rightarrow {}^4T_{2g}$ transition (see Supporting Information, Table S1).

The infrared spectra of **3** and **4** measured in KBr disks and in CH_2Cl_2, acetone, and methanol solutions (Table 9) are very similar to those of the analogous nickel complexes[17] and provide further support for the occurrence of both a carboxylate shift and a hydroxamate shift in **3** and **4** as suggested previously for the analogous nickel complexes. Thus while both **3** and **4** show peaks at 1626−1624 and 1603−1610 cm^{-1} in CH_2Cl_2 assigned to a bridging acetate and coordinated hydroxamate, respectively, there are again additional peaks at 1552 and 1558 cm^{-1} in **3** and **4**, respectively, which are absent in the KBr spectra and which are assigned to a carboxylate shift in which a bidentate acetate is in equilibrium with a monodentate bridging intermediate.[23] Similarly, **3** shows a new peak at 1613 cm^{-1} which again

Table 4. Selected Bond Lengths (Å) and Angles (deg) for Complex **4**

Co(1)−Co(2)	3.0971(6)	Co(1)−O(4)	2.060(2)
Co(1)−O(1)	2.045(3)	Co(1)−O(3)	2.170(2)
Co(1)−O(5)	2.121(2)	Co(1)−N(4)	2.248(3)
Co(1)−N(3)	2.175(3)	Co(2)−O(6)	2.070(2)
Co(2)−O(2)	2.040(3)	Co(2)−O(3)	2.183(2)
Co(2)−O(5)	2.088(2)	Co(2)−N(6)	2.226(3)
Co(2)−N(5)	2.195(3)		
O(1)−Co(1)−O(4)	176.61(11)	O(1)−Co(1)−O(5)	87.69(10)
O(4)−Co(1)−O(5)	93.60(10)	O(1)−Co(1)−O(3)	97.96(10)
O(4)−Co(1)−O(3)	79.15(9)	O(5)−Co(1)−O(3)	81.62(9)
O(1)−Co(1)−N(3)	90.08(12)	O(4)−Co(1)−N(3)	92.84(11)
O(5)−Co(1)−N(3)	98.09(11)	O(3)−Co(1)−N(3)	171.93(10)
O(1)−Co(1)−N(4)	88.12(13)	O(4)−Co(1)−N(4)	90.55(12)
O(5)−Co(1)−N(4)	175.76(11)	O(3)−Co(1)−N(4)	98.33(10)
N(3)−Co(1)−N(4)	82.56(12)	O(2)−Co(2)−O(6)	175.04(12)
O(2)−Co(2)−O(5)	95.69(11)	O(6)−Co(2)−O(5)	80.08(10)
O(2)−Co(2)−O(3)	90.07(10)	O(6)−Co(2)−O(3)	91.90(9)
O(5)−Co(2)−O(3)	82.08(9)	O(2)−Co(2)−N(5)	89.05(12)
O(6)−Co(2)−N(5)	95.15(12)	O(5)−Co(2)−N(5)	175.20(11)
O(3)−Co(2)−N(5)	98.73(10)	O(2)−Co(2)−N(6)	88.03(12)
O(6)−Co(2)−N(6)	89.89(11)	O(5)−Co(2)−N(6)	96.77(11)
O(3)−Co(2)−N(6)	177.67(11)	N(5)−Co(2)−N(6)	82.58(12)

Table 5. Selected Bond Lengths (Å) and Angles (deg) for Complex **5**

Co(1)−Co(2)	3.4128(11), 3.4219(11)	Co(1)−O(14)	2.060(4)
Co(1)−O(12)	2.059(4)	Co(1)−N(13)	2.172(5)
Co(1)−O(11)	2.083(4)	Co(1)−N(12)	2.212(6)
Co(1)−O(16)	2.210(4)	Co(2)−O(15)	2.063(4)
Co(2)−O(13)	2.031(4)	Co(2)−N(14)	2.168(6)
Co(2)−O(11)	2.071(4)	Co(2)−N(15)	2.230(6)
Co(2)−O(17)	2.184(4)	Co(3)−O(21)	2.070(4)
Co(3)−O(24)	2.055(4)	Co(3)−N(23)	2.153(5)
Co(3)−O(22)	2.083(4)	Co(3)−N(22)	2.240(5)
Co(3)−O(27)	2.192(4)	Co(4)−O(23)	2.057(5)
Co(4)−O(25)	2.036(4)	Co(4)−N(25)	2.166(6)
Co(4)−O(21)	2.081(4)	Co(4)−O(24)	2.230(6)
Co(4)−O(26)	2.199(4)		
O(12)−Co(1)−O(14)	96.79(18)	O(12)−Co(1)−O(11)	101.14(16)
O(14)−Co(1)−O(11)	89.57(16)	O(12)−Co(1)−N(13)	90.79(18)
O(14)−Co(1)−N(13)	89.83(19)	O(11)−Co(1)−N(13)	168.04(18)
O(12)−Co(1)−O(16)	175.51(17)	O(14)−Co(1)−O(16)	85.42(17)
O(11)−Co(1)−O(16)	74.91(16)	N(13)−Co(1)−O(16)	93.13(18)
O(12)−Co(1)−N(12)	89.1(2)	O(14)−Co(1)−N(12)	170.7(2)
O(11)−Co(1)−N(12)	96.3(2)	N(13)−Co(1)−N(12)	83.0(2)
O(16)−Co(1)−N(12)	89.19(19)	O(13)−Co(2)−O(15)	97.45(19)
O(13)−Co(2)−O(11)	99.14(17)	O(15)−Co(2)−O(11)	91.14(16)
O(13)−Co(2)−N(14)	90.0(2)	O(15)−Co(2)−N(14)	89.73(19)
O(11)−Co(2)−N(14)	170.65(19)	O(13)−Co(2)−O(17)	174.82(19)
O(15)−Co(2)−O(17)	84.72(18)	O(11)−Co(2)−O(17)	76.06(16)
N(14)−Co(2)−O(17)	94.75(19)	O(13)−Co(2)−N(15)	90.8(2)
O(15)−Co(2)−N(15)	169.11(19)	O(11)−Co(2)−N(15)	94.5(2)
N(14)−Co(2)−N(15)	83.2(2)	O(17)−Co(2)−N(15)	87.6(2)

is assigned to a "hydroxamate shift"[17] in which a monodentate bridging hydroxamate is in equilibrium with a form in which there is a weak interaction between the hydroxamate carbonyl oxygen and the metal center. The spectra in acetone and methanol show results similar to those in CH_2Cl_2 (Table 9).

Magnetic Susceptibility Measurements. The theoretical treatment of dinuclear Co(II) complexes belongs to one of the more difficult chapters of magnetochemistry. The Co(II) d^7 ion is strongly anisotropic, and the first-order orbital momentum is no longer negligible so the isotropic exchange interaction is insufficient to discuss these complexes and must be supplemented by considerations of orbitally dependent exchange interactions. This leads to invoking a large number of parameters to attempt a quantitative discussion of the temperature-dependent magnetic susceptibility data. Ideally, such data should be supplemented by complementary techniques, such as variable-temperature and variable-field magnetic circular dichroism; however, access to such techniques was not available so we have attempted to interpret the susceptibility data in terms of the minimum number of parameters which are physically meaningful.

(23) Rardin, L. R.; Tolman, W. B.; Lippard, S. J. *New J. Chem*. **1991**, *15*, 417−430.

Table 6. Selected Bond Lengths (Å) and Angles (deg) for Complex **8**

Co(1)−Co(2)	3.3466(7)	Co(1)−O(1)	1.889(3)
Co(1)−O(5)	1.873(3)	Co(1)−O(3)	1.916(3)
Co(1)−O(6)	1.899(3)	Co(1)−N(2)	2.071(3)
Co(1)−N(1)	2.019(3)	Co(2)−O(4)	2.064(3)
Co(2)−O(5)	1.997(3)	Co(2)−N(3)	2.191(3)
Co(2)−O(2)	2.104(3)	Co(2)−N(4)	2.206(3)
Co(2)−O(8)	2.199(4)		
O(5)−Co(1)−O(1)	90.61(13)	O(5)−Co(1)−O(6)	94.17(13)
O(1)−Co(1)−O(6)	175.16(12)	O(5)−Co(1)−O(3)	99.45(12)
O(1)−Co(1)−O(3)	90.88(12)	O(6)−Co(1)−O(3)	89.03(12)
O(5)−Co(1)−N(1)	89.23(13)	O(1)−Co(1)−N(1)	88.13(13)
O(6)−Co(1)−N(1)	91.23(13)	O(3)−Co(1)−N(1)	171.28(12)
O(5)−Co(1)−N(2)	176.40(13)	O(1)−Co(1)−N(2)	89.30(13)
O(6)−Co(1)−N(2)	85.88(13)	O(3)−Co(1)−N(2)	84.16(12)
N(1)−Co(1)−N(2)	87.17(13)	O(5)−Co(2)−O(4)	94.68(11)
O(5)−Co(2)−O(2)	88.70(11)	O(4)−Co(2)−O(2)	89.99(11)

Table 7. Selected Bond Lengths (Å) and Angles (deg) for Complex **7**

Co(1)−Co(2)	3.2635(5)	Co(1)−O(6)	1.8904(18)
Co(1)−O(5)	1.8819(19)	Co(1)−O(1)	1.9101(18)
Co(1)−O(3)	1.9029(17)	Co(1)−N(2)	2.029(2)
Co(1)−N(1)	2.023(2)	Co(2)−O(8)	1.8950(18)
Co(2)−O(5)	1.8681(18)	Co(2)−O(2)	1.9125(18)
Co(2)−O(4)	1.9025(17)		
O(5)−Co(1)−O(6)	89.53(8)	O(5)−Co(1)−O(3)	98.66(8)
O(6)−Co(1)−O(3)	95.81(8)	O(5)−Co(1)−O(1)	88.97(8)
O(6)−Co(1)−O(1)	177.02(8)	O(3)−Co(1)−O(1)	86.96(8)
O(5)−Co(1)−N(1)	88.51(9)	O(6)−Co(1)−N(1)	85.12(8)
O(3)−Co(1)−N(1)	172.77(9)	O(1)−Co(1)−N(1)	92.27(9)
O(5)−Co(1)−N(2)	175.23(9)	O(6)−Co(1)−N(2)	92.16(9)
O(3)−Co(1)−N(2)	85.61(8)	O(1)−Co(1)−N(2)	89.14(9)
N(1)−Co(1)−N(2)	87.19(9)	O(5)−Co(2)−O(8)	94.53(8)
O(5)−Co(2)−O(4)	95.05(8)	O(8)−Co(2)−O(4)	88.02(8)
O(5)−Co(2)−O(2)	90.54(8)	O(8)−Co(2)−O(2)	174.92(8)
O(4)−Co(2)−O(2)	91.82(8)		

Table 8. Selected Bond Lengths (Å) and Angles (deg) for Complex **9**

Co(1)−Co(2)	2.83	Co(1)−O(3)	1.895(4)
Co(1)−O(1)	1.905(4)	Co(1)−O(5)	1.893(4)
Co(1)−O(2)	1.906(4)	Co(1)−N(1)	2.027(5)
Co(1)−N(2)	2.031(5)	Co(2)−O(4)	1.909(4)
Co(2)−O(2)	1.897(4)	Co(2)−O(7)	1.897(4)
Co(2)−O(1)	1.903(4)	Co(2)−N(4)	2.024(5)
Co(2)−N(3)	2.026(5)		
O(1)−Co(1)−O(3)	88.37(18)	O(1)−Co(1)−O(2)	82.64(17)
O(3)−Co(1)−O(5)	175.17(18)	O(2)−Co(1)−O(3)	89.45(18)
O(2)−Co(1)−O(5)	94.11(18)		
O(1)−Co(1)−N(2)	86.96(8)	O(2)−Co(1)−N(2)	177.5(2)
O(5)−Co(1)−N(2)	88.3(2)	O(2)−Co(1)−N(1)	92.6(2)
O(1)−Co(1)−N(1)	173.9(2)	O(3)−Co(1)−N(1)	87.76(19)
O(5)−Co(1)−N(1)	88.8(2)	O(3)−Co(1)−N(2)	88.2(2)
O(2)−Co(1)−N(1)	88.1(2)	O(2)−Co(2)−O(7)	94.15(18)
O(2)−Co(2)−N(4)	94.4(2)	O(2)−Co(2)−O(1)	82.95(16)
O(2)−Co(2)−O(4)	89.72(18)	O(7)−Co(2)−O(1)	92.84(18)
O(6)−Co(2)−N(4)	88.14(8)	O(2)−Co(2)−O(4)	89.72(18)
O(5)−Co(2)−N(3)	172.74(8)	O(7)−Co(2)−O(4)	175.90(18)
O(4)−Co(2)−N(3)	86.72(8)	O(2)−Co(2)−N(4)	94.4(2)
O(5)−Co(2)−N(4)	92.29(8)	O(7)−Co(2)−N(4)	91.3(2)
O(4)−Co(2)−N(4)	170.53(9)	N(3)−Co(2)−N(4)	88.0(2)

Table 9. Infrared Spectral Data for Complexes **1**−**4** in Selected Solvents[a]

medium	2	3	1	4	assgnt
KBr	1669	1670			urea
	1618	1634	1630	1636	bidentate bridging acetate
		1606		1592,1610 (sh)	coord hydroxamate
	1559				monodentate acetate
CH_2Cl_2	1664	1663			urea
	1614	1626	1624	1624	bidentate bridging acetate
		1613			monodentate hydroxamate
		1603		1610	coord hydroxamate
	1553	1552	1557	1558	monodentate acetate
acetone	1669	1667			urea
	1617	1629	1632	1634	bidentate bridging acetate
		1604		1591, 1609	coord hydroxamate
	1550	1548	1554	1559	monodentate acetate
methanol	1666	1667			urea
	1627	1628		1627	bidentate bridging acetate
		1610		1582	coord hydroxamate
	1604				H-bonded acetate
	1560	1560	1562	1554	monodentate acetate

[a] All values in cm^{-1}.

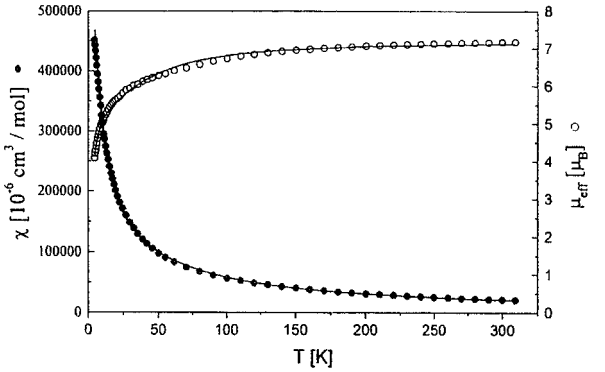

Figure 5. Susceptibility and effective magnetic moment per dimer vs temperature of complex $[Co_2(\mu\text{-}H_2O)(\mu\text{-}OAc)_2(OAc)_2(tmen)_2]$ (**1**). The solid lines represent the best fit with the following parameters: $J = -0.7$ cm^{-1}; $D = 45$ cm^{-1}, $g_{\|} = 2.9$; $g_{\perp} = 2.5$.

Complexes **1**−**3** were magnetically characterized by measuring the temperature dependence of their molar susceptibilities in the temperature range 4.4−310 K; the results for **4** were not reproducible. The behavior of the three complexes differs remarkably. While **3** shows a distinct maximum in χ_M at 15 K, **1** and **2** exhibit more or less a paramagnetic hyperbola. For all three compounds, the magnetic moment/dimer at room temperature is much higher than the spin-only value. In the case of **2**, the value increases on cooling from 7.61 μ_B at 300 K to 7.79 μ_B at 140 K followed by a decrease to 6.16 μ_B at 4.5 K. The effective magnetic moments of **1** and **3** decrease with decreasing temperature from 7.17 μ_B at 300 K to 4.08 μ_B at 4.6 K and from 7.20 μ_B at 300 K to 1.77 μ_B at 4.4 K, respectively. The temperature dependencies of the magnetic susceptibilities and effective magnetic moments of **1**−**3** are shown in Figures 5−7, respectively.

The magnetic data were interpreted in terms of the Hamiltonian: Here the first term is the isotropic exchange interaction

$$H = -2J\vec{S}_1\vec{S}_2 + \vec{S}_1\vec{D}_1\vec{S}_1 + \vec{S}_2\hat{D}_2\vec{S}_2 + \beta\vec{H}\hat{g}_1\vec{S}_1 + \beta\vec{H}\hat{g}_2\vec{S}_2$$

between two Co(II) ions, the next two terms are due to the local field splitting, and the last two terms are the Zeeman perturbation. The orbital contribution to the exchange interaction together with the biquadratic exchange and anisotropic exchange interactions have all been neglected. Calculations were performed on

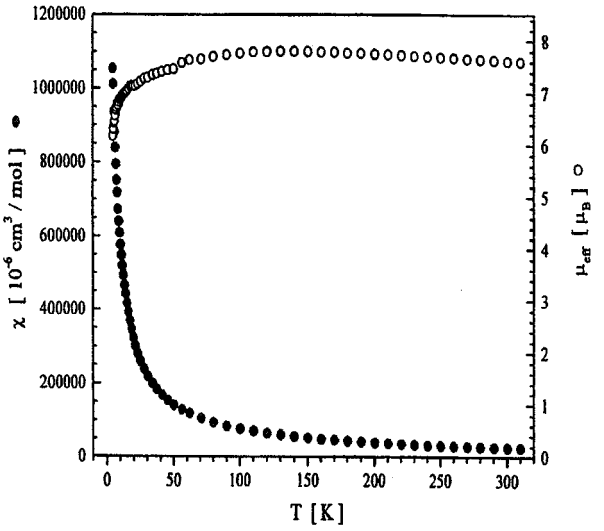

Figure 6. Susceptibility and effective magnetic moment per dimer vs temperature of complex $[Co_2(\mu\text{-}OAc)_3(urea)(tmen)_2][OTf]$ (**2**).

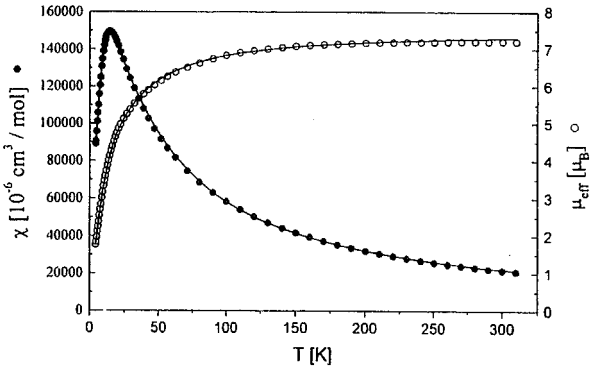

Figure 7. Susceptibility and effective magnetic moment per dimer vs temperature of complex $[Co_2(\mu\text{-}OAc)_2(\mu\text{-}AA)(urea)(tmen)_2][OTf]$ (**3**). The solid lines represent the best fit with the following parameters: $J = -3.6$ cm^{-1}; $D = 45$ cm^{-1}; $g_{\|} = 3.0$; $g_{\perp} = 2.6$.

a coupled basis, and the details are given elsewhere.[24] The principal values of the magnetic susceptibility were calculated from the usual expression:

$$\chi_u = NkT\frac{\partial^2}{\partial H_u^2}\left[\ln\sum_i \exp\left[\frac{-E_i(H_u)}{kT}\right]\right] \quad u = x_l y_l z$$

Here E_i are the energy levels of the system in the external magnetic field. Finally, the powder average susceptibility is calculated as

$$\chi_{av} = \frac{1}{3}(\chi_x + \chi_y + \chi_z)$$

The experimental magnetic properties of **1** as well as the calculated values of the magnetic susceptibility and effective magnetic moment are presented in Figure 5 (best-fit parameters are shown in the caption). The calculated value of the local axial zero field splitting parameter for **1** of $D = 45$ cm^{-1} is typical of high-spin Co(II). The small value of the isotropic exchange interaction ($J = -0.7$ cm^{-1}) indicates a very weak antiferromagnetic interaction consistent with the structure of **1** containing bridging acetate groups which do not provide a good pathway for superexchange. Due to this small value of the

(24) Ostrovski, S. M. Private Communication.

Table 10. Spectroscopic Data for Co^{III}_2 and $Co^{III}Co^{II}$ Dinuclear Homo- and Mixed-Valence Complexes

complex	IR carbonyl freq, cm^{-1}	UV/vis spectral data: λ_{max}, nm (ϵ, $cm^{-1}\ M^{-1}$) (CH_2Cl_2)
$[Co^{III}Co^{II}(\mu\text{-OH})(\mu\text{-OAc})_2(OAc)(urea)(tmen)_2][OTf]$ (**10**)	1670, 1618, 1560 (KBr) 1664, 1614, 1556 (CH_2Cl_2)	<368 (CT), 523 (74), 1093 (10)
$[Co^{III}_2(\mu\text{-OH})(\mu\text{-OAc})_2(OAc)(urea)(tmen)_2][OTf][OAc]$ (**11**)	1669, 1619, 1559 (KBr) 1665, 1615, 1554 (CH_2Cl_2)	<367 (CT), 377 (sh), 577 (126)
$[Co^{III}Co^{II}(\mu\text{-}H_2O)(\mu\text{-OH})(\mu\text{-OAc})(OAc)_2(tmen)_2][OAc]$ (**6**)	1631, 1548 (KBr) 1624, 1556, 1711 (CH_2Cl_2)	<450 (CT), 530 (66), 1093 (8)
$[Co^{III}_2(\mu\text{-OH})(\mu\text{-OAc})_2(OAc)_2(tmen)_2][OTf]$ (**7**)	1651, 1645, 1606, 1570 (KBr) 1655, 1645, 1604, 1568 (CH_2Cl_2)	<390 (CT), 383 (sh), 594 (281)
$[Co^{III}_2(\mu\text{-OH})(OH)(\mu\text{-OAc})_2(OAc)(tmen)_2][OTf]$ (**8**)	1632, 1576 (KBr) 1614, 1564,1554 (CH_2Cl_2)	<390 (CT), 380 (sh), 599 (293)
$[Co^{III}Co^{II}(\mu\text{-OH})(\mu\text{-OAc})_2(\mu\text{-AA})(urea)(tmen)_2][OTf][OAc]$ (**12**)	1670, 1633, 1607 (KBr)	<362 (CT), 525 (82), 1093 (9)

isotropic exchange parameter, the excited states with $M = \pm 1$ are very close in energy to the antiferromagnetic ground state and their thermal population is significant even at very low temperatures. Thus, at $T = 4.5$ K, the effective magnetic moment of **1** is about 4 μ_B. In contrast, the best-fit parameters for **3** give a J value of -3.6 cm^{-1} indicating a stronger antiferromagnetism than in **1** in accord with the presence of the bridging hydroxamate group although the analogous nickel complex shows a weak ferromagnetic interaction ($J = 4.09$ cm^{-1}).[17] Unfortunately, the magnetic properties of complex **2** cannot be explained within the framework of the above pure spin model. An analysis based on a model which takes into account a strong orbital contribution of Co(II) is in progress.

Dicobalt(III) Complexes 7−9. Oxidation of aqueous solutions of cobalt(II) in the presence of various ligands yields a range of μ-hydroxo and μ-peroxo complexes, for example, $[L_4Co(\mu\text{-OH})(\mu\text{-}O_2)CoL_4]^{3+}$ (L = NH_3, tn, tren, trien).[25] Dihydroxo- and trihydroxo-bridged dinuclear complexes together with mixed-valency Co(II)/Co(III) complexes have also been reported.[26] In view of the difficulty in assessing the protonation state of the bridging ligand in dinuclear metalloenzymes as mentioned in the Introduction, it was decided to attempt the synthesis of model dicobalt(III) complexes with bridging hydroxo groups by oxidation of the model dicobalt(II) complexes, **1**−**3** especially, since it was noted that, on prolonged exposure to air, pink solutions of **1** and **2** turned reddish-brown, indicating aerial oxidation.

Oxidation of solutions of the above complexes was attempted with a variety of oxidants such as $Ce(SO_4)_2$, HNO_3, air, and H_2O_2, but only with H_2O_2 were reproducible results obtained and only in the case of the oxidation of **1** and **3** were crystals obtained suitable for a structure determination, yielding complexes **7**−**9**.

Oxidation of 1 with H_2O_2. The dicobalt hydrolase model, **1,** reacted vigorously with hydrogen peroxide to give three products, one brown and two green, depending on the amount of hydrogen peroxide used. Addition of only a few drops of H_2O_2 to **1** in methanol gave after workup a brown complex **6** characterized by IR and UV−visible (Table 10). Its proposed structure shown in Scheme 1 of a mixed Co(II)/Co(III) bridged dimer. Excess of hydrogen peroxide added to a solution of **1** in methanol under nitrogen gave a green solution. Removal of solvent and treatment of the resulting green oil with diethyl ether and ethyl acetate gave two crystalline products, **8** and **7**, suitable for X-ray crystallography (Figures 8 and 9, respectively). Crystallographic data and selected bond lengths and angles are given in Tables 1, 6, and 7, respectively.

Scheme 1. Formation of Complexes **6**−**9** from the Oxidation of Complex **1** by H_2O_2[a]

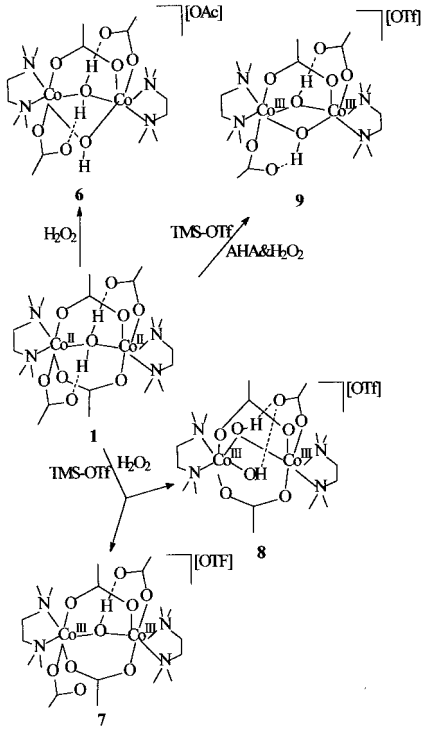

[a] Note: Complex **6** is a mixed Co(II)/Co(III) species.

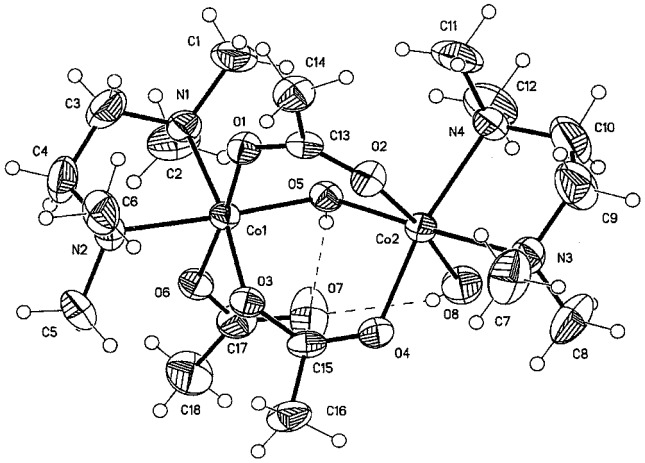

Figure 8. Molecular structure of the cation of dicobalt(III) complex **8**, $[Co_2(\mu\text{-OAc})_2(OAc)(\mu\text{-OH})(OH)(tmen)_2]^+$.

Both **7** and **8** contain a dicobalt(III) core with **8** containing both a terminal and a bridging hydroxo group together with bridging and monodentate acetates whereas **7** contains a single bridging hydroxo group. The Co−Co distances are 3.2635(5)

(25) Fallab, S.; Mitchel, P. R. *Adv. Inorg. Bioinorg. Mech.* **1984**, *3*, 311−377.

(26) Chaudhuri, P.; Querback, J.; Wieghardt, K.; Nuber, B.; Weiss, J. *J. Chem. Soc., Dalton Trans.* **1990**, 271−278.

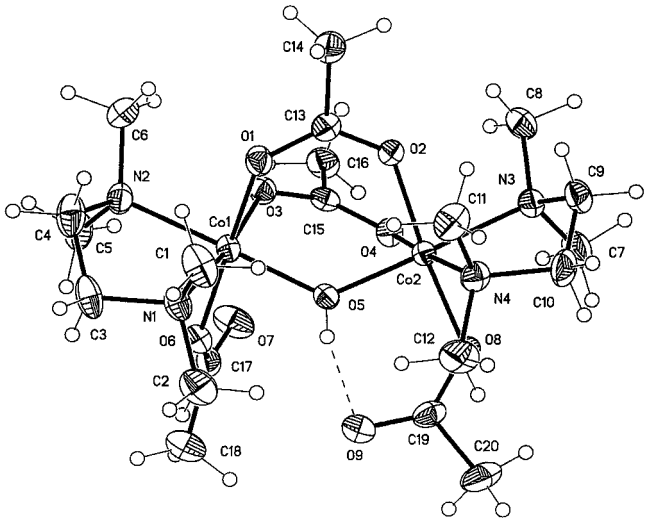

Figure 9. Molecular structure of the cation of dicobalt(III) complex **7**, $[Co_2(\mu\text{-}OAc)_2(OAc)_2(\mu\text{-}OH)(tmen)_2]^+$.

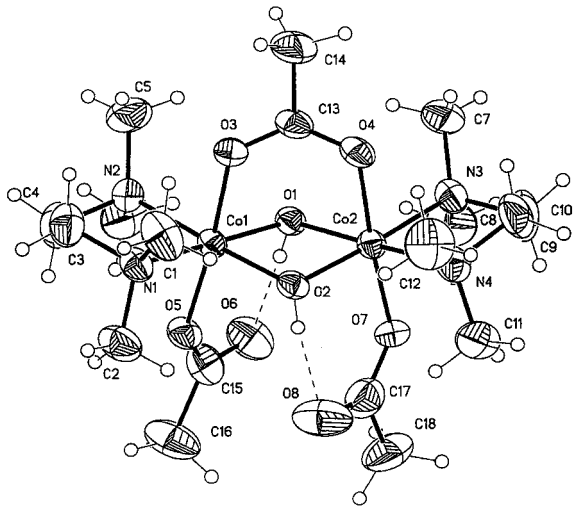

Figure 10. Molecular structure of the cation of dicobalt(III) complex **9**, $[Co_2(\mu\text{-}OAc)(OAc)_2(\mu\text{-}OH)_2(tmen)_2]^+$.

and 3.3466(7) Å in **7** and **8,** respectively, compared with a Co−Co distance of 3.597(11) Å in **1**.[20] As in the Co(II) dimers, the geometry about the cobalt centers is distorted octahedral. There is clear structural evidence for hydrogen bonding between both the bridging and terminal hydroxo groups and a monodentate acetate group.

The spectroscopic properties of **7** and **8** are in accord with the above crystal structures. Thus, the infrared spectra show clear evidence of both bridging and monodentate acetate groups (Table 10), while the electronic spectra of the green complexes (**7** and **8**) are very similar and close to those reported for the $[Co^{III}_2(\mu\text{-}OH)(\mu\text{-carboxylate})_2]^{3+}$ core[26] with a band in the region 599−560 nm assigned to the $^1A_{1g} \rightarrow {}^1T_{1g}$ transition and a shoulder in the region 380−390 nm assigned to the $^1A_{1g} \rightarrow {}^1T_{2g}$ transition. The formation of both **7** and **8** by oxidation of **1** suggests that **8** is formed sequentially from **7**, although the synthetic studies gave no evidence for this; however, NMR studies described below show that on standing, a solution of **7** in $CDCl_3$ developed peaks characteristic of **8.**

Formation of 8 from 7. When the ^{1}HNMR spectrum (see Supporting Information Tables S2−S4) of **7** ($CDCl_3$) was followed as a function of time, new peaks assigned to **8** appeared. For example the proton resonance of **7** at δ 9.42 due to the bridging OH decreases in intensity with time and concomitantly a proton resonance at δ 6.36 due to the terminal OH proton in **8** forms. Similar behavior occurs with the other proton signals. Further evidence for the formation of **8** from **7** is provided by the ^{13}C spectra where, in the carbonyl region of **7**, five rather than the expected four signals are observed (see Table S3); however, one of these lies at δ 187, the same value as in **8**. Clearly a solution of **7** in $CDCl_3$ equilibrates to form **8** with subsequent decomposition.

Reaction of 1 with TMS-OTf + AHA + H_2O_2. Reaction of **1** with AHA and hydrogen peroxide in the presence of TMS -triflate gave a dark green solution in methanol. Removal of solvent followed by extraction in chlorobenzene gave upon layering with ether dark green crystals of **9** suitable for X-ray crystallography. This complex contains a dicobalt(III) core and two bridging hydroxo groups (Figure 10 and Tables 1 and 8). It is noteworthy that, under these oxidative conditions, aceto-hydroxamic acid does not coordinate in the bridging mode which it adopts in the dicobalt(II) dimers **3** and **4** and in the related dinickel(II) complexes.[17] Complexes **7**−**9** are closely related and illustrate the ease of replacement of both bridging and terminal acetates by bridging and terminal hydroxy groups which show a marked propensity to hydrogen bond with any remaining suitably oriented acetate groups.

Oxidation of 2 with H_2O_2. Treatment of **2**, $[Co_2(urea)(\mu\text{-}OAc)_3(tmen)_2][OTf]$, with H_2O_2 in methanol gave two new complexes **10** and **11** depending on the amount of H_2O_2 used. If only one drop of H_2O_2 was used, a brownish solution formed immediately which on workup gave a brown solid **10** from which unfortunately crystals for X-ray diffraction could not be obtained. However, the microanalysis and infrared and electronic spectra (Table 10) suggest a mixed-valence Co(II)/Co(III) complex with a bridging hydroxo group and bridging and monodentate acetate groups as shown in Scheme 2.

In contrast, reaction of **2** with excess H_2O_2 gave after workup a dark green solid **11** and microanalysis, infrared and electronic spectroscopy suggest the structure shown in Scheme 2 with a Co^{III}_2 core, coordinated urea, bridging and monodentate acetates, and a bridging hydroxo group i.e., $[Co_2(\mu\text{-}OAc)_3(\mu\text{-}OH)(urea)(tmen)_2][OTf][OAc]$.

Thus, the infrared peak at 1669 cm^{-1} confirms retention of the coordinated urea. The electronic spectra of **10** and **11** are quite different. Thus, the spectrum of **10,** which is typical of the brown mixed-valence Co(II)/Co(III) complexes, gave a band in the near-infrared of low intensity in the region 1090−1093 nm and a stronger band around 520−530 nm (Table 10). The former is typical of Co(II), and the latter is found in both spectra of Co(II) and Co(III) complexes; however, the dicobalt(III) band at 520−530 nm is more intense than that in the dicobalt(II) and is accompanied by a CT peak below 350 nm which is absent in the dicobalt(II) complexes and in some cases a shoulder at ∼380 nm is also reported. In contrast, the spectrum of **11** is typical of the dinuclear Co(III) complexes containing a bridging hydroxo group and is close to those of **7** and **8** (see Supporting Information Table S1 and Table 10).

Reaction of 3 with H_2O_2. When an excess of complex **3**, $[Co_2(\mu\text{-}AA)(\mu\text{-}OAc)_2(urea)(tmen)_2][OTf]$, was reacted with H_2O_2, a brown product, **12**, was formed which is assigned the structure shown in Scheme 2 on the basis of microanalysis and infrared and electronic spectra.

In all the above compounds, attempts to measure their Raman spectra were unsuccessful because of decomposition in the laser beam. Finally, attempts to promote the hydrolysis of urea with these hydroxo-bridged complexes were unsuccessful, not surprisingly in view of the relative inertness of Co(III) complexes

Scheme 2. Oxidation of **2** and **3** with H_2O_2 and Formation of Complexes **10**−**12**[a]

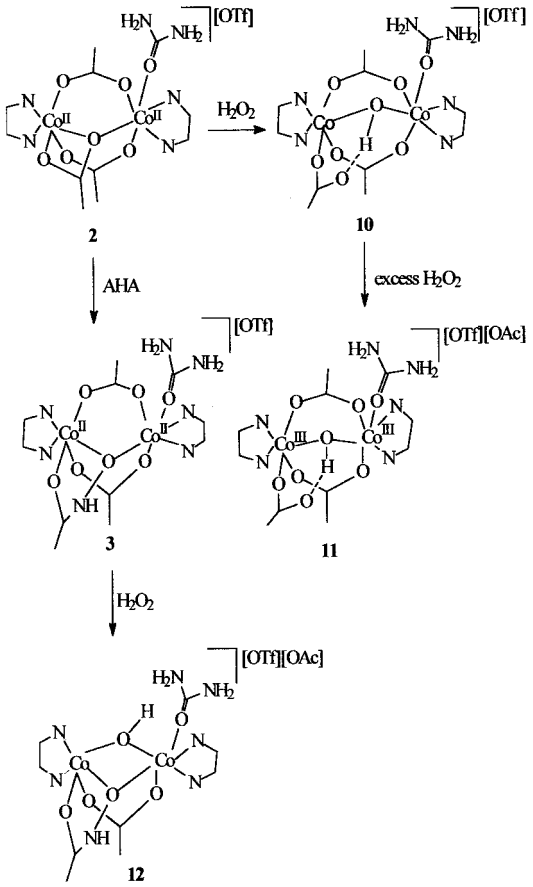

[a] Note: Complexes **10** and **12** are mixed Co(II)/Co(III) species. <

compared to Co(II) complexes. In contrast, preliminary studies indicate that complex **6** reacts rapidly with amide substrates while complex **7** shows catalase type reactivity with H_2O_2. Further studies of these reactions are in progress.

Experimental Section

Solvents were freshly purified by standard methods. Reagents were used directly without purification. Infrared spectra were measured as KBr disks on a Perkin-Elmer Paragon 1000 Fourier transform spectrometer. UV/ visible spectra were measured in dichloromethane solution on a Perkin-Elmer Lamba 6 UV/vis spectrometer. ^{1}HNMR spectra were recorded on Varian INOVA 300 and Varian INOVA 500 MHz spectrometers. ^{13}C NMR spectra were obtained on a Varian INOVA 300 MHz spectrometer and a Varian INOVA 500 MHz spectrometer operating at 75 and 126 MHz, respectively. Chemical shifts are reported downfield from tetramethylsilane (TMS) as internal reference. Elemental analyses were performed by the Microanalytical Unit of the Chemistry Services Unit of University College, Dublin.

Preparation of Hydroxamic Acids. Acetohydroxamic acid and glutarodihydroxamic acid were prepared as described previously.[27, 28]

Preparation of Parent Cobalt Complex 1. $[Co_2(\mu\text{-}H_2O)(\mu\text{-}OAc)_2(OAc)_2(tmen)_2]$ was prepared by the literature method.[20]

Preparation of Cobalt Complex 2: $[Co_2(\mu\text{-}OAc)_3(urea)(tmen)_2][OTf]$. Complex **1** (5.03 g, 8.33 mmol) was dissolved in dry dichloromethane (30 mL) and stirred with 1.50 mL (1.85 g, 8.33 mmol) of (trimethylsilyl)triflate for 1 h. Urea (1.0 g, 16.7 mmol) was then added and stirring continued for 12 h. Excess urea was filtered off, and vapor diffusion of diethyl ether into the filtrate gave dark pink crystals of **2** (3.98 g, 5.41 mmol, yield 65%). Anal. Calcd for $Co_2C_{20}H_{45}N_6O_{10}SF_3$ (**2**): C, 32.61; H, 6.16; N, 11.41. Found: C, 32.33; H, 6.01; N, 11.36.

Preparation of Monobridged Acetohydroxamate Complex 3: $[Co_2(\mu\text{-}OAc)_2(\mu\text{-}AA)(urea)(tmen)_2][OTf]$. Complex **2** (368 mg, 0.500 mmol) and acetohydroxamic acid (AHA) (37.5 mg, 0.500 mmol) were stirred in dichloromethane (2 mL) until a clear solution resulted. Layering with *n*-pentane or 2,2-dimethoxypropane gave pink crystals of **3**, $[Co_2(urea)(OAc)_2(\mu\text{-}AA)(tmen)_2][OTf]$ (yield 0.200 mmol, 40%). Anal. Calcd for $Co_2C_{20}H_{46}O_{10}N_7SF_3$ (**3**): C, 31.96; H, 6.13; N, 13.05. Found: C, 31.78; H, 6.10; N, 12.99.

Preparation of Dibridged Acetohydroxamate Complex 4: $[Co_2(\mu\text{-}AA)_2(\mu\text{-}OAc)(tmen)_2][OTf]$. Complex **1** (302 mg, 0.500 mmol) and acetohydroxamic acid (AHA) (75 mg, 1.00 mmol) were dissolved in acetone in the presence of 0.18 mL (1.00 mmol) of triflate and stirred for 1 h. Evaporation of the acetone gave an oil which dissolved in a dichloromethane−acetone mixture (1:1), and layering of this with petroleum ether gave pink crystals of **4**, $[Co_2(\mu\text{-}AA)_2(\mu\text{-}OAc)\ (tmen)_2][OTf]$ (yield 0.195 mmol, 39%). Anal. Calcd for $Co_2C_{19}H_{45}N_6O_{10}SF_3$ (**4**): C, 32.30; H, 6.14; N, 11.90. Found: C, 32.14; H, 6.00; N, 11.72.

Preparation of Complex 5: $[Co_2(\mu\text{-}OAc)_2\{(\mu\text{-}O(N)(CO)_2(CH_2)_3\}(tmen)_2][OTf]$. Complex **1** (604 mg, 1 mmol) was dissolved under nitrogen in dry methanol (5 mL) and triflate (0.18 mL, 1.00 mmol) injected. After the solution was stirring for 1 h, glutarodihydroxamic acid ($gluH_2A_2$) (180 mg, 1.00 mmol) dissolved in dry methanol (2 mL) was added. After this solution was stirring for 30 min, solvent was removed and the resulting oil dissolved in dichloromethane which, on layering with *n*-pentane, gave dark pink crystals of **5** (yield 0.35 mmol, 35%). Anal. Calcd for $Co_2C_{22}H_{44}N_5O_{10}SF_3$: C, 35.44; H, 5.94; N, 9.39. Found: C, 35.01; H, 5.77; N, 9.16.

Reaction of 2 with H_2O_2. When **2** (368 mg, 0.5 mmol) was treated with 0.067 mL of H_2O_2 (27%) (0.6 mmol) in methanol, the color of the solution changed from pink to brown. A brown oil was obtained upon removal of the solvent under reduced pressure. Treatment of the oil with light petroleum or diethyl ether gave the brown product complex $[Co^{III}Co^{II}(\mu\text{-}OH)(\mu\text{-}OAc)_2(OAc)(urea)(tmen)_2][OTf]$ (**10**) (yield 0.42 mmol, 84%). Anal. Calcd for $Co_2C_{20}H_{46}N_6O_{11}SF_3$: C, 31.88; H, 6.15; N, 11.15. Found: C, 32.17; H, 5.97, N, 11.07.

Reaction of 2 with Excess H_2O_2. When **2** (368 mg, 0.5 mmol) was treated with 0.27 mL of H_2O_2 (27%) (2.4 mmol) in methanol, a green solution was obtained accompanied by large changes in the UV−visible spectrum of the solution. Removal of the solvent afforded a green oily residue which gave a solid green product, complex **11,** $[Co_2(OAc)_3(OH)(urea)(tmen)_2][OTf][OAc]$, upon treatment with a minimum amount of an ethyl acetate/ether mixture (yield 0.38 mmol, 0.28 g, 75%). Anal. Calcd for $Co_2C_{22}H_{49}O_{13}N_6SF_3$ (**11**): C, 32.52; H, 6.10; N, 10.34; Co, 14.51. Found: C, 31.06; H, 5.85; N, 11.09; Co, 15.88.

Reaction of 2 with AHA and H_2O_2. When compound **2** (736 mg, 1.00 mmol) was reacted with AHA (75 mg, 1.00 mmol) in methanol and the resulting pink solution treated with 0.14 mL (1.2 mmol) of H_2O_2 (27%), a brown solution formed which upon workup gave the brown solid complex $[Co^{III}Co^{II}(\mu\text{-}OAc)(\mu\text{-}AA)(\mu\text{-}OH)(urea)(tmen)_2][OTf][OAc]$ (**12**) (yield 0.78 mmol, 78%). Anal. Calcd for $Co_2C_{20}H_{47}O_{11}N_7SF_3$: C, 31.84; H, 6.28; N, 11.13; Co, 15.62. Found: C, 30.88; H, 5.94; N, 12.74; Co, 14.62.

Reaction of 1 with H_2O_2. 1 (604 mg, 1.0 mmol) in methanol was reacted with 0.12 mL (1.0 mmol) of H_2O_2 (27%). Removal of solvent afforded the brown solid complex **6** (yield 0.95 mmol, 95%). Anal. Calcd for $Co_2C_{20}H_{47}O_{10}N_4$ (**6**): C, 38.65; H, 7.65; N, 9.01; Co, 18.5. Found: C, 38.15; H, 7.43; N, 8.89; Co, 19.2.

Reaction of 1 with Excess H_2O_2. 1 (602 mg, 1 mmol) was reacted with 1 mmol of TMS-OTf (0.18 mL) in methanol and the resulting solution stirred for 1 h. Addition of 0.28 mL (2.5 mmol) of H_2O_2 (27%) resulted in a bright green solution. Removal of the solvent afforded a dark green oil. Treatment of this oil with diethyl ether extracted a yellowish green solution and a dark green oily solid. After separation, the dark green oily solid was treated with ethyl acetate and gave upon layering with ethyl benzene good quality dark green crystals of the

(27) Brown, D. A.; Roche, A. L. *Inorg. Chem.* **1983**, *22*, 2199−2202.
(28) Brown, D. A.; Coogan, R. A.; Fitzpatrick, N. J.; Glass, W. K.; Abukshima, D. E.; Shiels, L.; Ahlgren, M.; Smolander, K.; Pakkanen, T. T.; Pakkanen, T. A.; Peräkyla, M. J. *J. Chem. Soc., Perkin Trans. 2* **1996**, 2673−2679.

complex **7** suitable for X-ray analysis (yield 0.38 mmol, 38%). Anal. Calcd for $Co_2C_{21}H_{45}N_4O_{12}SF_3$ (**7**): C, 33.51; H, 6.03; N, 7.44; Co, 15.66.

Found: C, 33.40; H, 5.96; N, 7.35; Co, 15.79. The above ether solution also gave good quality green crystals suitable for X-ray analysis of complex **8** (yield 0.19 mmol, 19%). Anal. Calcd for $Co_2C_{19}H_{43}N_4O_{11}SF_3$ (**8**): C, 32.12; H, 6.10; N, 7.88; Co, 16.59. Found: C, 31.62; H, 6.12; N, 7.46; Co, 17.00.

Reaction of 1 + OTf + AHA + H_2O_2 Excess. **1** (604 mg, 1 mmol) was reacted with 1 mmol of TMS-OTf (0.18 mL) in methanol. To this solution AHA (150 mg, 2.00 mmol) was added followed by H_2O_2 (0.28 mL, 2.5 mmol) resulting in a change of color of the solution from pink to green. Removal of solvent, treatment of the resulting oil with chlorobenzene, and layering with diethyl ether gave shiny dark green crystals of complex $[Co^{III}_2(\mu\text{-OH})_2(\mu\text{-OAc})(OAc)_2(tmen)_2][OTf]$ (**9**) suitable for X-ray crystallography

(yield 0.32 mmol 32%). Anal. Calcd for $Co_2C_{19}H_{43}N_4O_{11}SF_3$ (**9**): C, 32.12; H, 6,10; N, 7.88; Co, 16.59. Found: C, 31.59; H, 5.82; N, 7.69; Co, 18.79.

Treatment of Complexes 7 and 8 with Urea. When 0.5 mmol of **7** or **8** was treated with excess urea in the presence or the absence of TMS-triflate, no change was observed in the UV−vis spectrum or IR spectrum in methanol, even after overnight stirring. Filtration and removal of the solvent gave an oil, from which the starting materials were recovered intact.

Treatment of 7 and 8 with Hydroxamic Acids. When 0.5 mmol of **7** was mixed with AHA (0.5 mmol) in CH_2Cl_2, no reaction was observed, and the starting material was obtained after workup. The same result was observed for complex **8**.

Treatment of 7 and 8 with Urea and AHA. When the cobalt(III) complexes formed by reacting **1** with excess H_2O_2 were mixed with urea and AHA, no changes were seen in either the UV−Vis or the IR spectra indicating that the complexes are inactive to these substrates.

Crystals Structure Determinations of Complexes 2−5 and 7−9. Crystals suitable for X-ray analysis were obtained directly from the above preparation methods. Data were collected using a Siemens SMART CCD area-detector diffractometer. A full hemisphere of reciprocal space was scanned by a combination of three sets of exposures; each set had a different ϕ angle for the crystal, and each exposure of 10s covered 0.3° in ω. The crystal to detector distance was 5.01 cm. Crystal decay was monitored by repeating the initial frames at the end of the data collection and analyzing the duplicate reflections; a multiscan absorption correction was applied using SADABS.[29]

The structures were solved by direct methods using SHELXTL-PC[30] and refined by full-matrix least-squares on F^2 for all data using SHELXL-97.[31] Hydrogen atoms were added at calculated positions and refined using a riding model.[31]Anisotropic temperature factors were used for all non-H atoms; H atoms were given isotropic temperature factors equal to 1.2 (or 1.5 for methyl hydrogens) times the equivalent isotropic displacement parameter of the atom to which the H atom is attached. In the case of **5**, there were two formula units in the asymmetric unit and one of the triflates is highly disordered.

Magnetic Measurements. The magnetic susceptibilities of powdered samples of **1**−**3** were recorded on a Faraday-type magnetometer consisting of a Cahn RG electrobalance, a Leyboldt Heraeus VNK 300 helium flux cryostat, and a Bruker BE25 magnet connected with a Bruker B-Mn 200/60 power supply in the temperature range 4.4−310 K. The applied magnetic field was about 1.5 T. Details of the apparatus have been described elsewhere.[32,33] The experimental susceptibility data were corrected for underlying diamagnetism in the usual manner using Pascal's constants.[34] Corrections for diamagnetism were estimated as -376.2×10^{-6}, -339.0×10^{-6}, and -380.1×10^{-6} cm^3/mol for **2**, **1,** and **3**, respectively.

Conclusions

The ability of the dicobalt model hydrolase $[Co_2(\mu\text{-}H_2O)(\mu\text{-}OAc)_2(OAc)_2(tmen)_2]$ (**1**) to form a cobalt-based urease model complex $[Co_2(\mu\text{-}OAc)_3(urea)(tmen)_2][OTf]$ (**2**) and to cause hydroxylamine elimination from glutarodihydroxamic acid and form $[Co_2(\mu\text{-}OAc)_2\{\mu\text{-}O(N)\ (OC)_2(CH_2)\}(tmen)_2][OTf]$ (**5**) in a manner identical to that for the nickel-based urea models[17,18] gives strong support to a close similarity between Co(II) and Ni(II) in dinuclear-based metalloenzymes. This similarity can probably be extended to other divalent metal ions utilized in metalloenzymes such as Zn(II) and Mn(II).[35]

The facile replacement of both carboxylate groups and water molecules, a common structural feature of dinuclear metalloenzymes, by acetohydroxamic acid in the model compounds **1** and **2** to form bridged hydroxamate cobalt complexes with essentially the same structures as their nickel analogues suggests that hydroxamic acids can also inhibit cobalt-based hydrolases as well as inhibiting urease.

Oxidation of the dicobalt(II) complexes **1**−**3** gave a series of mixed Co(II)/Co(III) dimers as intermediates in the formation of Co(III) dimers containing both bridging and terminal hydroxy groups. In contrast to the dicobalt(II) series, acetohydroxamic acid does not form bridged complexes with the dicobalt(III) series of complexes. Oxidation occurs by ready replacement of acetate groups with formation of the hydroxy complexes.

Acknowledgment. We are pleased to acknowledge the support of the EUCOST program, Project D8/0010/97.

Supporting Information Available: Tables of analytical data and infrared and electronic spectra of complexes **1**−**12** together with NMR data (^{1}H, ^{13}C) for complexes **7** and **8** and relevant assignments. This material is available free of charge via the Internet at http://pubs.acs.org.

IC0103345

(29) Sheldrick, G. M. *SADABS, Emprirical Absorption Corrections Program*; University of Göttingen: Göttingen, Germany, 1996.
(30) Siemens. *SHELXTL-PC Version 5.0 Reference Manual*; Siemens Industrial Automation, Inc., Analytical Instrumentation: Madison, WI, 1994.
(31) Sheldrick, G. M. *SHELLXL97 Program for Crystal Structure Refinement*; University of Göttingen: Göttingen, Germany, 1997.
(32) Merz, L.; Hasse. W. *J. Chem. Soc., Dalton Trans*. **1980**, 875−879.
(33) Gehring, S.; Fleischhauer; Paulus, H.; Haase, W. *Inorg. Chem*. **1993**, *32*, 54−60.
(34) Kahn, O. *Molecular Magnetism*; VCH Publishers: New York, 1993.
(35) **Note Added in Proof:** A bridging hydroxamate has also been confirmed for manganese by crystallographic studies of $[Mn_2(OAc)_3(AA)(tmen)_2]$ prepared in these laboratories from the reaction of $[Mn_2(OAc)_4(H_2O)(tmen)_2]$ and AHA.